American Journal of Nanoscience and Nanotechnology
2013;1(1): 1-5
Published online May 20, 2013 (http://www.sciencepublishinggroup.com/j/nano)
doi: 10.11648/j.nano.2013.0101.11

Fabrication and characterization of ZnO nanostructures on Si (111) substrate using a thin ALN buffer layer

L.S. Chuah[1]*, Z. Hassan[2], S. K. Mohd Bakhori[2], M. A. Ahmad[2], Y. Yusof[2]

[1] Physics Section, School of Distance Education, Universiti Sains Malaysia, 11800 Penang, Malaysia
[2] School of Physics, Universiti Sains Malaysia, 11800 Penang, Malaysia

Email address:
chuahleesiang@yahoo.com (L.S. Chuah)

To cite this article:
L.S. Chuah, Z. Hassan, S. K. Mohd Bakhori, M. A. Ahmad, Y. Yusof. Fabrication and characterization of ZnO nanostructures on Si(111) substrate using a thin AlN buffer layer. *American Journal of Nanoscience and Nanotechnology.* Vol. 1, No. 1, 2013, pp. 1-5.
doi:10.11648/j. nano.2013.0101.11

Abstract: In the present work, radio-frequency (RF) nitrogen plasma-assisted molecular beam epitaxy (PA-MBE) technique was used to grow AlN thin layers on Si (111) substrate. Subsequently, the thermal evaporation technique was used to deposit the zinc films on Si(111) substrates with AlN as buffer layer. ZnO nanostructures were obtained from zinc granulated (99.99%) by thermal oxidation from 400 °C to 600 °C in air for 1 hours without any catalysts. The effect of annealing temperatures were studied ranging from 400 °C to 600 °C in air for 1 hours. The AlN was introduced to accommodate the lattice mismatch and thermal expansion mismatch between ZnO layer and Si substrate. The structural and optical properties of ZnO nanostructures are studied through scanning electron microscopy (SEM), X-ray diffraction (XRD) and room temperature photoluminescence (PL) spectroscopy. The films show a polycrystalline hexagonal wurtzite structure without preferred (0002) orientation. The mean grain sizes are calculated to be about 18 nm, 22 nm and 50 nm for the ZnO films prepared at temperatures of 400 °C, 500 °C and 600 °C. The structure of the fabricated nanomaterials were characterized by scanning electron microscopy (SEM). The PL spectra of the ZnO nanostructures having a sharp excitonic ultraviolet (UV) emission and very weak defect-related deep level visible emissions. It is showed that the ZnO nanostructures thermal annealed treatment was performed at 600 °C shows the strongest UV emission intensity among the temperatures ranges studied. In addition, from the one-dimensional ZnO nanostructures thermal annealed at 600 °C, the stronger UV emission is assigned to the best crystalline quality of the ZnO film.

Keywords: Nanostructures, ZnO, AlN, Si, Thermal evaporation, SEM, XRD, PL

1. Introduction

Wide-bandgap (WBG) semiconductor thin films (diamond, GaN, AlN and SiC), have develop into the focal spot of intense research focus in photonics and optoelectronics in the past decade because of an increasing require for short wavelength (200-250nm) optoelectronic devices [1-3].

Zinc oxide (ZnO) is a promising material for ultraviolet (UV) optoelectronics, as in reality it has a few primary benefits over the III-V semiconductors. The fundamental band gap of ZnO is 3.37 eV or 375 nm at room temperature, and a large exciton binding energy of ZnO (60 meV) among the II-VI semiconductors and make possible the realization of low-threshold lasing in ZnO [4-7].

There are various kinds to synthesize nanostructures of ZnO such as vapor phase methods [8-10] and solution phase methods [11]. Conventionally, gold (Au) and silver (Ag) were explored as a catalyst for the growth of ZnO one dimentional nanowire. However, this process may cause contamination problems. In other report, other metal catalyst coatings, for example Pt, Cu, and Pd, have also been reported.

Recent year, unlimited of the study has well-defined on fabricating of different morphologies of ZnO nanostructures for example nanorod, nanoneedle, nanobow, nanowall, nanobridge, nano-tetrapod and nano-multipod nanostructures [10-15]. Those nanostructures not only given powerful instruments for investigating crystal growth at a nanoscale, but they also showed promising sight for fabricating achievement improved unique nanoelectronic devices [16]. In the different morphologies of ZnO nanostructures, such as tetrapod, tetraneedle and multipod nanostructures have attracted huge observations [17, 18].

The multipod nanostructures of ZnO have novel applications in both functional and structural materials because of their optical, electrical and optoelectronic properties [19].

Despite high quality bulk ZnO substrates are available over growth, their high cost and restricted reasonable actually impede their used in large output. Nevertheless, sapphire is high-priced, insulating and bound in size. But silicon, is an attractive substrate due to its low cost, good thermal stability and conductivity, high crystalline quality, and availability of large diameter silicon wafers. By chance, it was shown that the mismatch of lattice constants (15%) and thermal expansion coefficients (56%) between ZnO and Si(111) are truly large. Consequently, growth of high quality ZnO films on Si(111) will be a numerous challenge [20]. In the existing work, we applied a thin AlN buffer layer to grow ZnO nanostructure and relatively small lattice mismatch to ZnO. The thermal expansion coefficient of AlN is in the average between thermal expansion coefficient of ZnO and silicon. With all these characteristics recommend that AlN will be a suitable buffer for ZnO films grown on Si (111) substrates.

2. Experiment

AlN was grown on Si (111) substrate using Veeco model Gen II MBE system for 15 minutes [21]. High purity material sources for examples aluminum (6N5) was used in the Knudsen cells. Nitrogen (7N purity) was channeled to RF source to create reactive nitrogen species. The plasma was operated at typical nitrogen pressure of 1.5×10^{-5} Torr under a discharge power of 300 W at 13.56 MHz radio frequency (RF).

The growth of AlN on Si (111) substrate starts with the standard cleaning procedure by using a standard Radio Corporation of America (RCA) cleaning method prior to loading into MBE load lock chamber. In the preparation chamber, the substrates were outgassed for 10 min at 400 °C prior to growth. The growth chamber was equipped with a cryopump and the base pressure of the growth chamber was in the range of 10^{-11} Torr. The cryopump, drifted by a helium compressor with a water-cooling system, was commonly maintained at 10 Kelvin and hold the pressure of the growth chamber in the range of 10^{-11} Torr. In the growth chamber, Si substrate was heated at 840 °C, and then a few monolayers of Ga were deposited on the substrate for the purpose of removing the SiO_2.

Then a few monolayer of Al is deposited on silicon prior to the AlN buffer layer growth. It is famous that this buffer layer plays critical function in determining the crystalline quality of the thin film. To grow AlN buffer layer, substrate temperature was heated up to 845 °C, both of the Al and N shutters were opened simultaneously for 15 minutes [21].

Afterward, the thermal evaporation method was applied to coat the zinc (Zn) films on AlN buffer layer. The influence of annealing temperatures ranging from 400 °C to 600 °C in air for 1 hours. The as-synthesized ZnO nanostructures were characterized by using scanning electron microscopy (SEM). To evaluate the crystalline structure and the quality of the sample, high-resolution PANalytical X'Pert Pro MRD XRD system was used. Photoluminescence (PL) measurements were performed at room temperature using Jobin Yvon HR800UV system. He-Cd (325 nm) laser were used as excitation sources for PL measurement.

3. Results and Discussion

Zn thin films were deposited by thermal evaporation method on (111) n-Si substrates with AlN as buffer layer. Figure 1 shows the X-ray diffraction (XRD) spectra of the ZnO films prepared by oxidizing zinc films in air at temperatures of 400 °C. The samples present polycrystalline crystal structure without preferential orientation. No diffraction patterns of other materials are detected.

The indexed diffraction peaks in the pattern can be assigned to pure hexagonal phase ZnO. Four peaks appear at 2θ from 30° to 70° in the spectra of the ZnO films, and they correspond to the (002), (101), (102), and (201) directions of the hexagonal ZnO crystal structure. Moreover, the obvious and fine diffraction peaks also indicated that the as-synthesized products are pure obtain a high crystalline quality of the ZnO nanostructures.

No diffraction peaks from other impurities have been detected. The strong sharp (002) peak of ZnO wurtzite structure and much weaker (100) and (101) peaks are because of the incomplete vertical growth of the nanostructures. The specific growth mechanism undoubtedly requires advance studies.

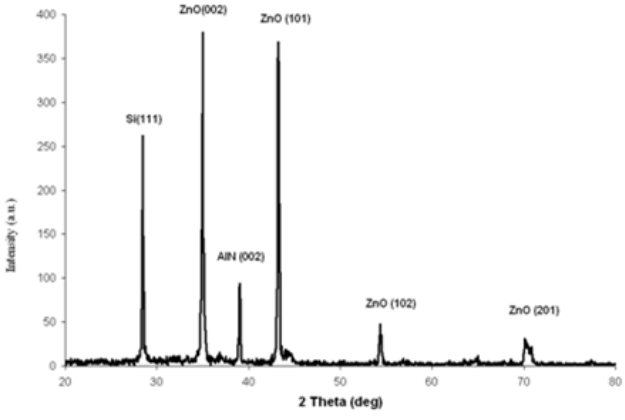

(a) 400 °C

Fig 1. *XRD spectra of ZnO nanostructures prepared at different temperatures.*

The average grain size in the films can be estimated by the Scherrer formula using the full width at half maximum

(FWHM) value of the XRD diffraction peaks. The Scherrer formula is

$$D = 0.9 \lambda / B \cos \theta \quad (1)$$

where *D, λ, θ, and B* are the main grain size, the X-ray wavelength of 0.154 nm, Bragg diffraction angle, and the FWHM of the diffraction peak of the (002) ZnO films [22]. The mean grain sizes are calculated to be about 18 nm, 22 nm and 50 nm for the ZnO films prepared at temperatures of 400 °C, 500 °C and 600 °C. The XRD peak can also be broadened via internal stress and defects.

Typical SEM micrograph of the surface of AlN/Si thin layer is illustrated in figures 2. From figure 3, their crystal structure features were characterized using X-ray diffraction (XRD). The surface morphologies of the ZnO films vary highly with an increase in oxidation temperature. At oxidation temperature of 600 °C (Fig 3d), the film consist of ZnO nanostructures throughout the polycrystalline matrix. In the films, however, the nanorods are dispersed in a matrix having a grain size ranging between 80 and 100 nm. Their density is much higher in this film. This would develop the surface energy and result favours the nucleation of [002] oriented grains [23]. The growth direction of ZnO nanorods is described to be [002]. It can be seen from Fig. 2b, that many ZnO nanostructures were distributed randomly on the silicon (111) substrates. No cracks are observed in the film.

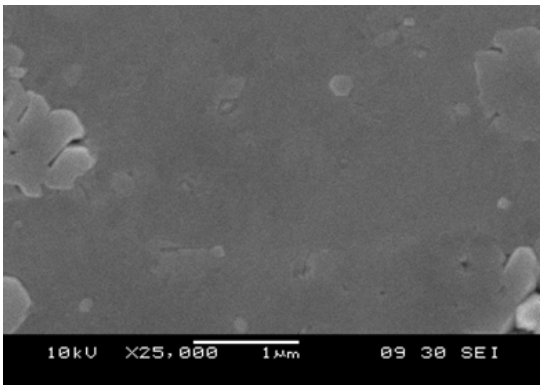

Fig 2. *Microscopic image for the AlN/Si (111) template.*

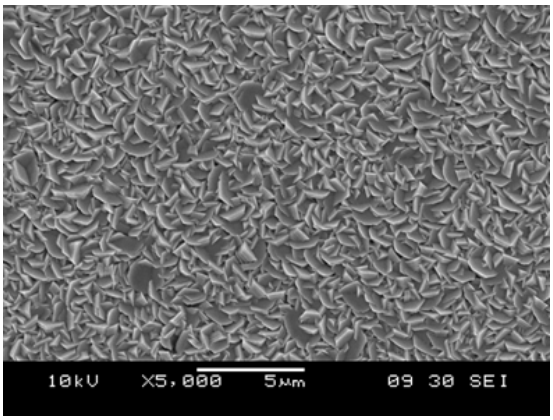

(a) As deposited Zn film on AlN/Si (111).

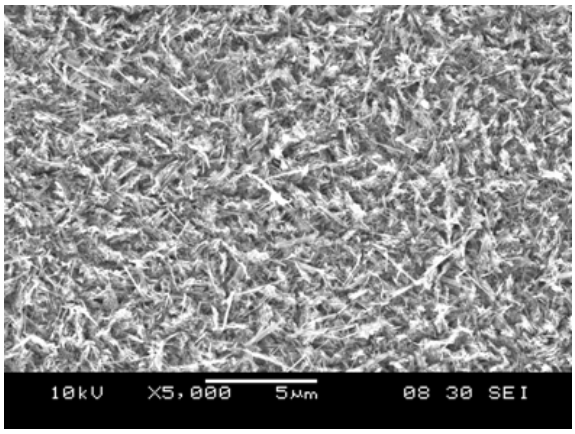

(b) ZnO films prepared at 400 °C.

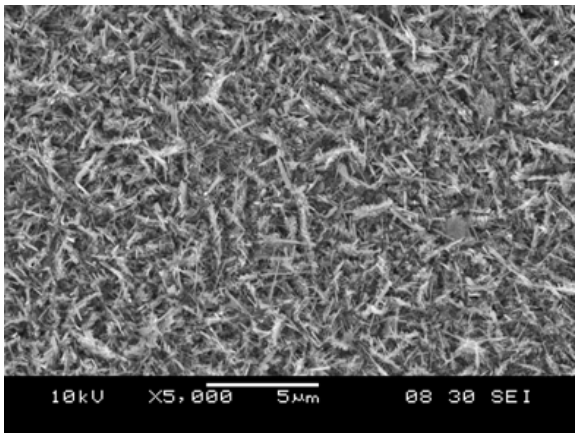

(b) ZnO films prepared at 500 °C.

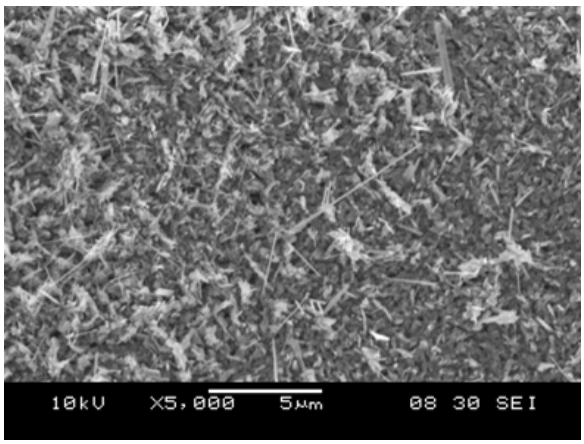

(d) ZnO films prepared at 600 °C.

Fig 3. *SEM photographs showing the morphology of the ZnO film grown on AlN/Si(1 1 1) template.*

Energy dispersive X-ray (EDX) analysis (in the SEM) was applied to study the composition of ZnO structures. The spectrum for the case of ZnO structures. Zinc and oxygen are the only observable components, supporting the view that no other metal elements are aiding in catalyzing the observed nanostructures growth.

The photoluminescence (PL) property of the ZnO structures is one of the most important properties that has

been investigated. The room temperature PL spectra of the as-synthesized ZnO nanostructures is given in Fig. 4. It can be seen that the PL spectra composed of two emission bands: a strong ultraviolet (UV) band at □380 nm, and a green emission band are centered at □520nm. The UV emission is introduced from the exitonic recombination analogous to the near band edge (NBE) emission of band gap ZnO, indicating the growth of good quality ZnO nanostructures [24]. The shape of all the spectra, similar to those reported by others [25-26], are dominated by strong near edge UV emission and defect related deep level emission. The UV emission peak originates from free excitonic emission as presented by other researchers [27], and it can be seen from Fig. 4.

We observed a green light emission peak at □520 nm, commonly referred to a deep-level or trap-state emission [28]. The deep level emission in ZnO may be ascribed to the solely ionized oxygen void in the ZnO nanostructures and the consequences from the recombination of electrons at the conduction band (CB) with holes captured in oxygen-associated defects [25]. However, it is well known that ZnO easily produces intrinsic defects such as interstitial zinc (Zn_i) and oxygen vacancy (V_O). These defects will affect the photoluminescence manner of ZnO in distinct ways [29]. In this work, in the process of the tetrapod-like ZnO nanostructures are grown at 600 °C in the air, an amount of oxygen vacancies can simply be formed. Thus, the green emission at □520 nm would be a result of the existence of the oxygen vacancies in the ZnO nanostructures.

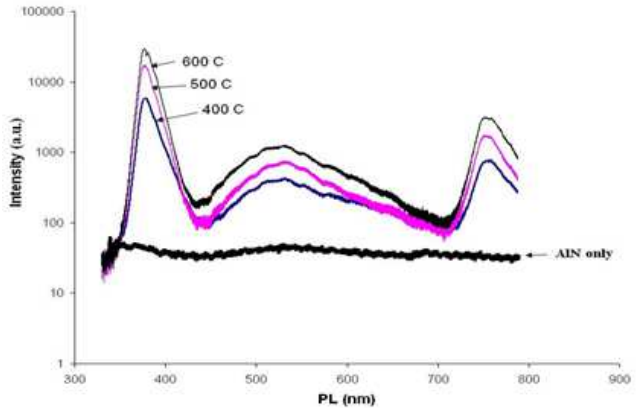

Figure 4. *The PL spectra obtained from the surfaces of the ZnO structures.*

4. Conclusions

The ZnO nanostructures were synthesized on Zn-coated Si (111) substrates by using a thin AlN buffer layer. The structure and particle size were determined by using XRD. SEM and PL analyses show that the nanostructures are pure wurtzite structure ZnO. Room-temperature PL spectrum of the ZnO nanostructures shows a UV emission peak at □380 nm and a green emission peak at □ 520 nm, which can be assigned to the near band edge emission and the deep level emission.

Acknowledgements

The authors would like to acknowledge Universiti Sains Malaysia and FRGS for financial support.

References:

[1] A. Nahhas, H. Koo Kim, Appl. Phys. Lett. 78 (2001) 1151.

[2] Y.F. Chen, F.Y. Jiang, L. Wang, C.D. Zheng, J.N. Dai, Y. Pu, W.Q. Fang, J. Crystal Growth 275 (2005) 486.

[3] Y. Chen, H.-J. Ko, S.-K. Hong, T. Yao, Appl. Phys. Lett. 76 (2000) 559.

[4] G. Chai, O. Lupan, L. Chow, H. Heinrich, Crossed zinc oxide nanorods for ultraviolet radiation detection, Sens. Actuators A: Phys. 150 (2009) 184.

[5] H. Kind, H. Yan, B. Messer, M. Law, P. Yang, Nanowire ultraviolet photodetectors and optical switches, Adv. Mater. (Weinheim, Ger.) 14 (2002) 158.

[6] C.H. Liu, W.C. Yiu, F.C.K. Au, J.X. Ding, C.S. Lee, S.T. Lee, Electrical properties of zinc oxide nanowires and intramolecular p–n junctions, Appl. Phys. Lett. 83 (2003) 3168.

[7] D.C. Reynolds, D.C. Look, B. Jogai, Optically pumped ultraviolet lasing from ZnO, Solid State Commun. 99 (1996) 873.

[8] O. Lupan, L. Chow, G. Chai, B. Roldan, A. Naitabdi, A. Schulte, H. Heinrich, Nanofabrication and characterization of ZnO nanorod arrays and branched microrods by aqueous solution route and rapid thermal processing, Mater. Sci. Eng. B: Solid 145 (2007) 57.

[9] N. Wang, Y. Cai, R.Q. Zhang, Growth of nanowires, Mater. Sci. Eng. R 60 (2008) 1–51.

[10] T. Pauporte, G. Bataille, L. Joulaud, F.J. Vermersch, Well-aligned ZnO nanowire arrays prepared by seed-layer-free electrodeposition and their Cassie–Wenzel transition after hydrophobization, J. Phys. Chem. C 114 (1) (2010) 194.

[11] O. Lupan, L. Chow, G. Chai, L. Chernyak, O. Lopatiuk-Tirpak, H. Heinrich, Focused-ion-beam fabrication of ZnO nanorod-based UV photodetector using the in-situ lift-out technique, Phys. Stat. Sol. A 205 (2008) 2673.

[12] X. Teng, H. Fan, S. Pan, C. Ye, G. Li, Abnormal photoluminescence of ZnO thin film on ITO glass, Mater. Lett. 61 (2007) 201–204.

[13] K. Keem,H. Kim, G.T. Kim, J.S. Lee, B. Min, K. Cho, M.Y. Sung, S. Kim, Photocurrent in ZnO nanowires grown from Au electrodes, Appl. Phys. Lett. 84 (2004) 4376.

[14] M. Guo, P. Diao, X.D. Wang, S.M. Cai, The effect of hydrothermal growth temperature on preparation and photoelectrochemical performance of ZnO nanorod array films, J. Solid State Chem. 178 (2005) 3210.

[15] N.O.V. Plank, I. Howard, A. Rao, M.W.B. Wilson, C. Ducati, R.S. Mane, J.S. Bendall, R.R.M. Louca, N.C. Greenham, H. Miura, R.H. Friend, H.J. Snaith, M.E. Welland, Efficient ZnO nanowire solid-state dye-sensitized solar cells using organic dyes and core–shell nanostructures, J. Phys. Chem. C 113 (2009) 18515–18522.

[16] C.H. Ku, J.J. Wu, Electron transport properties in ZnO nanowire array/ nanoparticle composite dye-sensitized solar cells, Appl. Phys. Lett. 91 (2007) 093117.

[17] C.Y. Jiang, X.W. Sun, G.Q. Lo, D.L. Kwong, J.X. Wang, Improved dye-sensitized solar cells with a ZnO-nanoflower photoanode, Appl. Phys. Lett. 90 (2007) 263501.

[18] J.B. Baxter, A.M.Walker, K. van Ommering, E.S. Aydil, Synthesis and characterization of ZnO nanowires and their integration into dye-sensitized solar cells, Nanotechnology 17 (2006) S304–S312.

[19] H. Gao, G. Fang, M. Wang, N. Liu, L. Yuan, C. Li, L. Ai, J. Zhang, C. Zhou, S. Wu, X. Zhao, The effect of growth conditions on the properties of ZnO nanorod dye-sensitized solar cells, Mater. Res. Bull. 43 (2008) 3345–3351.

[20] L. Wang, Y. Pu, Y.F. Chen, C.L. Mo, W.Q. Fang, C.B. Xiong, J.N. Dai, F.Y. Jiang, Journal of Crystal Growth 284 (2005) 459-463.

[21] L.S. Chuah, Z. Hassan, H. Abu Hassan, The growth of AlN thin films on Si(111) substrate by plasma-assisted molecular beam epitaxy, *Optoelectronics and Advanced Materials-Rapid Communications*, Vol. 2, No. 3, 137-139 (2008).

[22] R.J. Hong, H.J. Qi, J.B. Huang, H.B. He, Z. X. Fan, J. Shao, Influence of oxygen partial pressure on the structure and photoluminescence of direct current reactive magnetron sputtering ZnO thin films, *Thin Solid Film*, 473, 58-62 (2005).

[23] S. Cho, J. Ma, Y. Kim, G. K. L. Wong, and J. B. Ketterson, Photoluminescence and ultraviolet lasing of polycrystalline ZnO thin films prepared by the oxidation of the metallic Zn, *Appl. Phys. Lett*., 75, 2761-2763 (1999).

[24] L.Feng, A. Liu, M. Liu, Y. Ma, J. Wei, B. Man, Fabrication and characterization of tetrapod-like ZnO nanostructures prepared by catalyst-free thermal evaporation, *Mater. Character.* 61, 128-133 (2010).

[25] A. Toumiat, S. Achour, A. Harabi, N. Tabet, M. Boumaour, M. Maallemi, Effect of nitrogen reactive gas on ZnO nanostructure development prepared by thermal oxidation of sputtered metallic zinc, *Nanotech.,* 17, 658-663 (2006).

[26] S. J. Chen, Y. C. Liu, J.G. Ma, D.X. Zhao, Z. Z. Zhi, Y. M. Lu, J. Y. Zhang, D. Z. Shen, X. W. Fan, High-quality ZnO thin films prepared by two-step thermal oxidation of the metallic Zn, *J. Cryst. Growth,* 240, 467-472 (2002).

[27] F.K. Shan, B.C. Shin, S.W. Jang, Y.S. Yu, Substrates effects of ZnO thin films prepapred by PLD technique, *J. Eur. Cer. Soc.*, 24, 1015-1018 (2004).

[28] L.S. Chuah, Z. Hassan, S. S. Tneh, H. Abu Hassan, Porous silicon as an intermediate buffer layer for zinc oxide nanorods, *Composite Interfaces* 17, 733-742 (2010).

[29] M. Yang, Z.B. Huang, G. F. Yin, X. M. Liao, Y.D. Yao, Y.Q. Kang, J.W. Gu, Effect of thermal treatment on the structure and optical properties of biomimic hierarchical ZnO column arrays, *J Alloys Comp*, 495, 275- 279 (2010).